

Title: **Repairability Performance and Restoring Force Characteristics of Damaged H-shaped Steel Members after Repair**

Authors: Kenjiro Mori, Tokyo University of Science
Takumi Ito, Tokyo University of Science
Hanako Sato, Tokyo University of Science
Hiroka Munemura, Tokyo University of Science
Takeshi Matsumoto, Tokyo University of Science
Changhoon Choi, Tokyo University of Science

Subject: Structural Engineering

Keywords: Steel
Structure

Publication Date: 2015

Original Publication: International Journal of High-Rise Buildings 2015 Number 1

Paper Type:

1. Book chapter/Part chapter
2. **Journal paper**
3. Conference proceeding
4. Unpublished conference paper
5. Magazine article
6. Unpublished

© Council on Tall Buildings and Urban Habitat / Kenjiro Mori; Takumi Ito; Hanako Sato; Hiroka Munemura; Takeshi Matsumoto; Changhoon Choi

Repairability Performance and Restoring Force Characteristics of Damaged H-shaped Steel Members after Repair

Kenjiro Mori[†], Takumi Ito, Hanako Sato, Hiroka Munemura,
Takeshi Matsumoto, and Changhoon Choi

Tokyo University of Science, 6-3-1 Nijuku, Katsushika-ku, Tokyo, Japan

Abstract

Recently, new keywords such as “Resilience” and “Repairability” have been discussed from the perspective of the sustainability of damaged structures after a severe disaster. To evaluate the repairability and recovery of structures, it is necessary to establish an analytical method that can simulate the behavior of repaired structures. Furthermore, it is desirable to establish an evaluation method for the structural performance of repaired structures. This study investigates the repairability and recovery of steel members that are damaged by local buckling or cracks. This paper suggests a simple analytical model for repaired steel members, in order to simulate the inelastic behavior and evaluate the recoverability of the structural performance. There is good agreement between the analytical results and the test results. The proposed analytical method and model can effectively evaluate the recoverability.

Keywords: Steel structure, Repairability, Failure mode, Repair method, Damaged steel member

1. Introduction

Recently, there have been many discussions about repairability and recovery for damaged building structures after severe disasters. In particular, there has been a focus on the new keyword “RESILIENCE”, which represents the revival potential or function maintenance of damaged structures. Moreover, because of projected environmental and resource problems in the near future, there is interest in reusing and recycling old or used structural members. Considering these global trends, the establishment and maintenance of techniques and design methods concerned with the concept of resilience has become increasingly important.

A technical guideline and design procedure for repairing damaged buildings has been established by the Japan building disaster prevention association (JBDPA manual). Based on past research, for example, Tanaka et al. (1990) experimentally studied to develop a repair method following local buckling for steel members in steel structures after a disaster, the JBDPA manual contains several methods to repair structural members that have been damaged by seismic loads, and criteria to estimate the structural performance of repaired members. Fig. 1 shows repair methods following local buckling for steel members, in an H-shaped steel beam and a thin-walled box steel

column.

Significant research has suggested reinforcement for members with poor resistant performance. However, the relationship between repair method and repairability has not been well reported.

To evaluate the precise performance of repaired steel structures after a disaster, methods that can quantify the structural performance of the repaired members are needed. In this study, a horizontal loading test was conducted to experimentally verify the effect of existing repair methods in the JBDPA manual. Based on the experimental test result, an analytical model for steel members following repair is proposed, and an analytical study is conducted in order to simulate the inelastic behavior and evaluate to what extent the structural performance can be recovered.

2. Details of Repair Methods

2.1. Repair method for cracks

The JBDPA manual mentions the repair method for cracks, in which the damaged area is generally replaced with a renewal member. However, it is considered that local buckling and residual plastic deformation would disturb replacing a damaged member by a renewal member.

Therefore, this paper suggests a method for repairing cracks that occur around the intersection part of a flange and web. Fig. 2 outlines the repair method for H-shaped steel members that have cracks. The repair procedure is as follows:

[†]Corresponding author: Kenjiro Mori
Tel: +81-3-5876-1717 (Ex. 1711); Fax: +81-3-3609-7367
E-mail: spy54tv9@theia.ocn.ne.jp

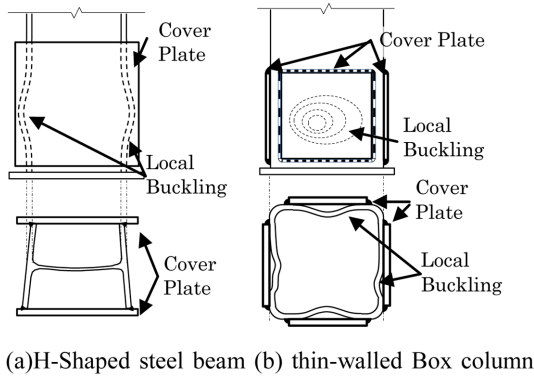


Figure 1. Repair methods for local buckling.

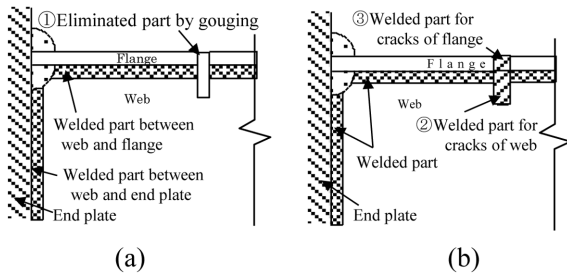


Figure 2. Detail of the method for repairing cracks: (a) Remove cracks; (b) Repair cracks by welding.

1. The area around the crack is removed by gouging
2. The removed area of web is filled by welding.
3. The removed area of flange is filled by welding.

2.2. Repair method for local buckling

The JBDPA manual proposes a method for repairing the damaged area caused by local flange buckling of H-shaped steel members. In this method, the damaged area is repaired by welding cover plates to the flanges, as shown in Fig. 3. In accordance with the JBDPA manual, a clearance of 25 mm is opened between the end plate and the edge of the cover plates. The thickness of the cover plates is equal to that of the flange plate of the H-shaped steel members.

3. Horizontal Loading Test

3.1. General description

In this study, horizontal loading tests were performed to verify the effects of the repair methods. Table 1 summarizes the test specimens, and Table 2 lists the mechanical properties of steel. The test specimens are set up as cantilever beams, as shown in Fig. 4, and a lateral load is applied to the top of the specimens. The configurations of the test specimens are shown in Fig. 5.

The outline of loading test is explained as follows. First, specimens that have been damaged with local buckling or

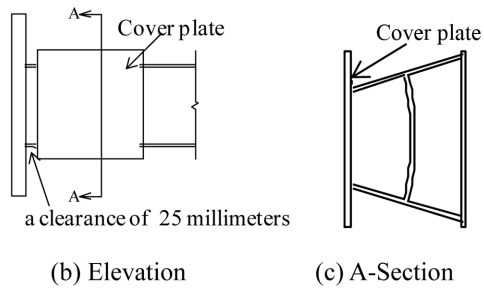
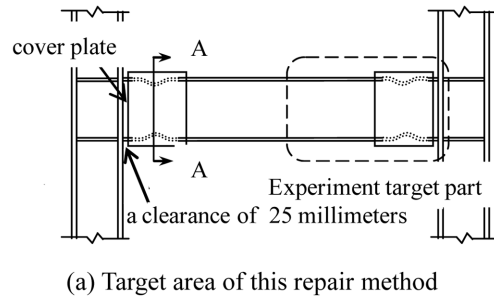


Figure 3. Detail of the method of repairing damaged area with local buckling.

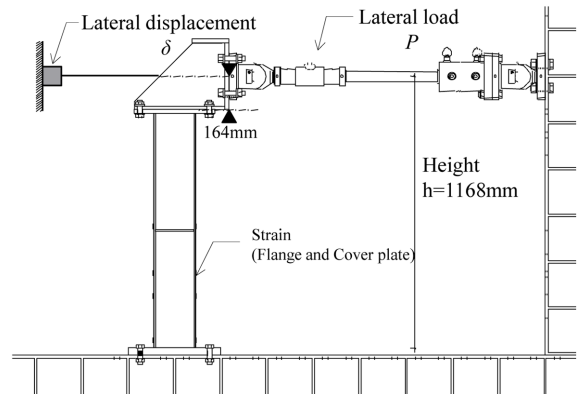


Figure 4. Test setup.

cracks are produced by a horizontal loading test (First-loading test). Next, the deformed and damaged test specimens are returned to the original position (Returning). Then, the damaged part around the local buckling and cracks is repaired by the methods described in Section 2. Finally, the loading tests are conducted again on the repaired test specimens (Second-loading test), using the same loading history as the first loading tests. The test specimens were instrumented with sensors to measure the lateral displacement at the top of the test specimens, and the strain of the flange and cover plates.

3.2. Experimental parameters

In this paper, the presence of scallop, depth-thickness ratio of steel members, and loading history are considered

Table 1. List of test specimens

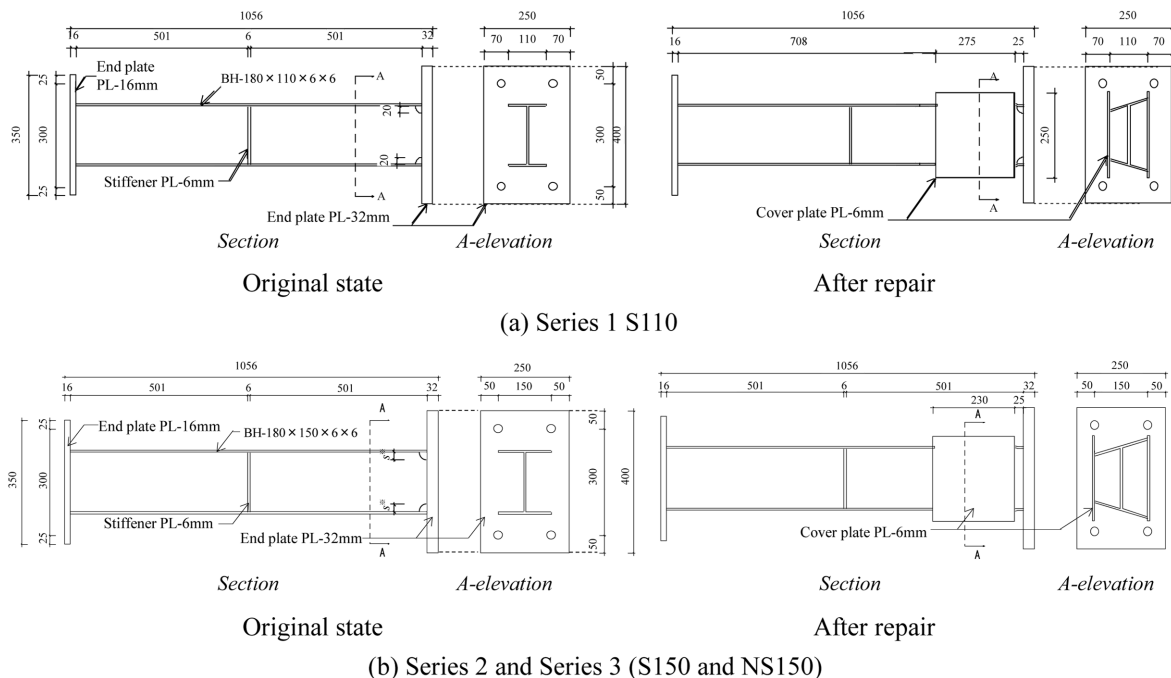
Series	Specimens	Section	b/t_f^*	d/t_w^*	Scallop size	Steel grades**	Repair	Loading history
Series 1	S110-NM	BH-180×110×6×6	8.67	28.0	20	SM490	unrepair	monotonic
	S110-RM							monotonic
	S110-R1						repair	cyclic1
	S110-R2							cyclic2
	S110-R3							cyclic3
Series 2	S150-NM	BH-180×150×6×6	12.0	28.0	20	SM490	unrepair	monotonic
	S150-RM							monotonic
	S150-R4						repair	cyclic4
	S150-R5							cyclic5
	S150-R6							cyclic6
Series 3	NS150-NM	BH-180×150×6×6	12.0	28.0	Non Scallop	SM490	unrepair	monotonic
	NS150-RM							monotonic
	NS150-R7						repair	cyclic7
	NS150-R8							cyclic8
	NS150-R9							cyclic9

* b/t is the width-thickness ratio of flange, d/t is the width-thickness ratio of web.

**Grade of JIS (Japanese Industrial Standards).

Table 2. Mechanical properties of steel

Series	Parts	Steel grades (Grade of JIS)	Thickness (mm)	Yield strength (N/mm ²)	Tensile strength (N/mm ²)	Young's modulus (GPa)
Series 1				387	541	213
Series 2	Web and Flange	SM490	6	387	541	213
Series 3				390	544	217


Figure 5. Configuration of test specimens.

as parameters.

Three kinds of test specimens, series 1-3, are prepared

in the loading test. Series 1 and 2 have scallop (see Fig. 4), which is representative of steel members in older existing

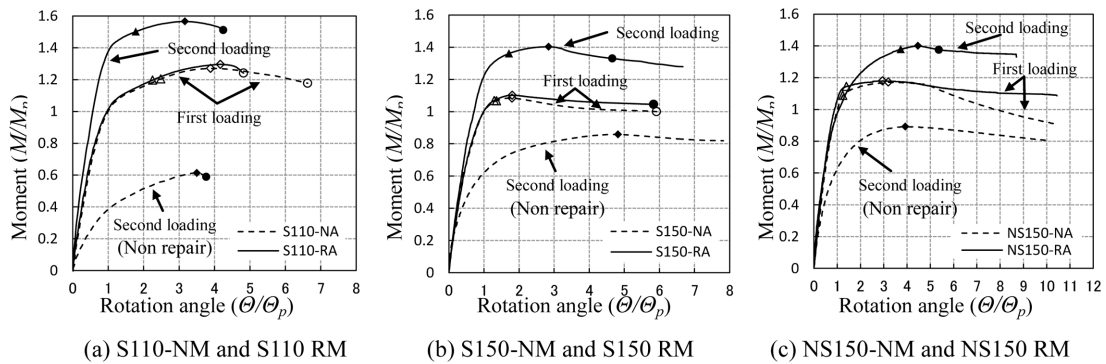


Figure 6. Comparison of normalized $M-\theta$ curve of monotonic loading.

structures. The width-thickness ratio of series 1 is different from other series. In the Japanese seismic resistance code, series 1 (BH-180×110×6×6) is classified as FB rank, whereas series 2 and 3 (BH-180×150×6×6) are classified as FC rank. The loading histories are divided into four patterns for each series, as shown in Table 1. For each series, monotonic loading is applied to two specimens, and cyclic loading to the remainder.

3.3. Experimental results

Fig. 6 shows the normalized moment-rotation angle curves ($M-\theta$ curve) under monotonic loading, and Figs. 7-9 show the $M-\theta$ curves under cyclic loading test. The moment M is normalized by the fully plastic moment M_p , and the angle θ is normalized by θ_p , the rotation angle at which the load reaches M_p for monotonic loading. Triangle symbols indicate local buckling, rhombus symbols indicate maximum strength, and circle symbols indicate the occurrence of cracks.

Table 3 compares the test results before and after the repair process. M_m is the maximum strength, η_m is the energy absorption capacity up to the maximum load, and

“Failure mode” is the dominant factor of maximum strength determination.

3.3.1. Monotonic loading

In all specimens, local buckling occurred during the load increasing process, before the load reached maximum strength. Subsequently, the first-loading test ended after a crack occurred or the load sufficiently deteriorated.

In the case of S110-NM and S110-RM before repair, they have higher strength and ductility than S150-NM and S150-RM because of the different width-thickness ratio. In the case of NS150-NM and NS150-RM before repair, they have higher strength and ductility than S150-NM and S150-RM, because cracks did not occur in NS150-NM and NS150-RM.

During the second-loading test (after repair), all specimens showed a significant increase in maximum strength under monotonic loading, and the ductility had recovered until the load reached maximum strength. In the test of specimens S110-RM and NS150-RM after repair, it was observed that local buckling initiated at the upper area of cover plates, and subsequently the load reached maximum

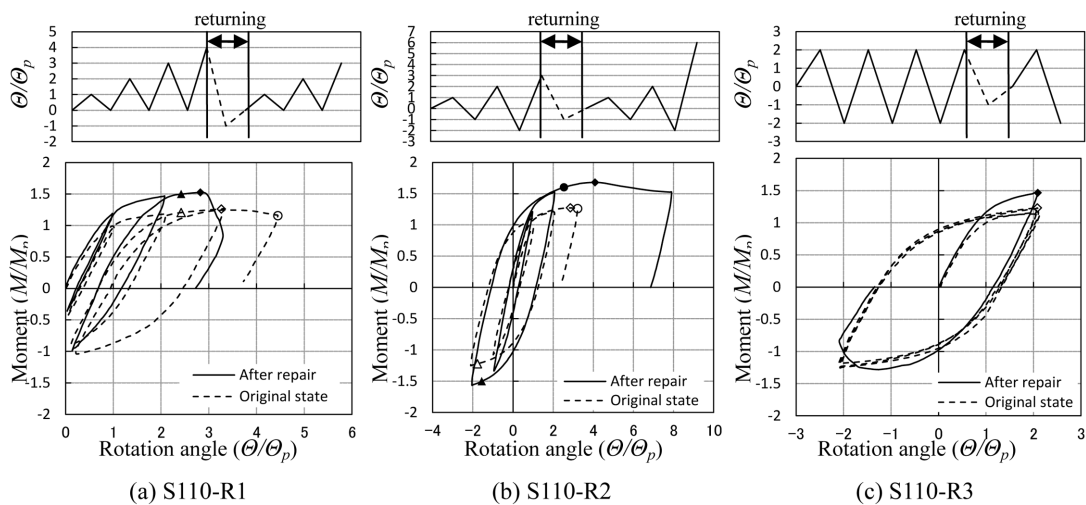


Figure 7. Comparison of normalized $M-\theta$ curve of cyclic loading of the specimens series 1.

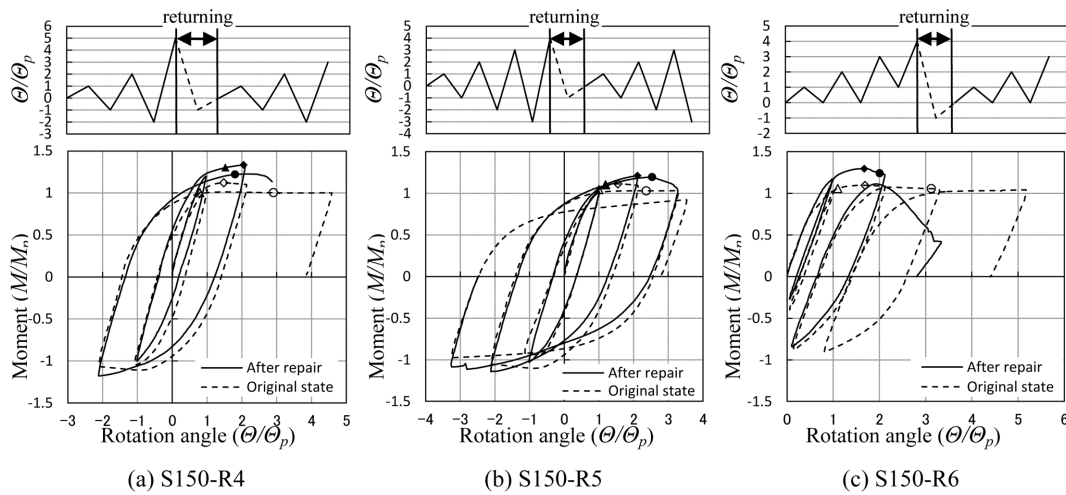
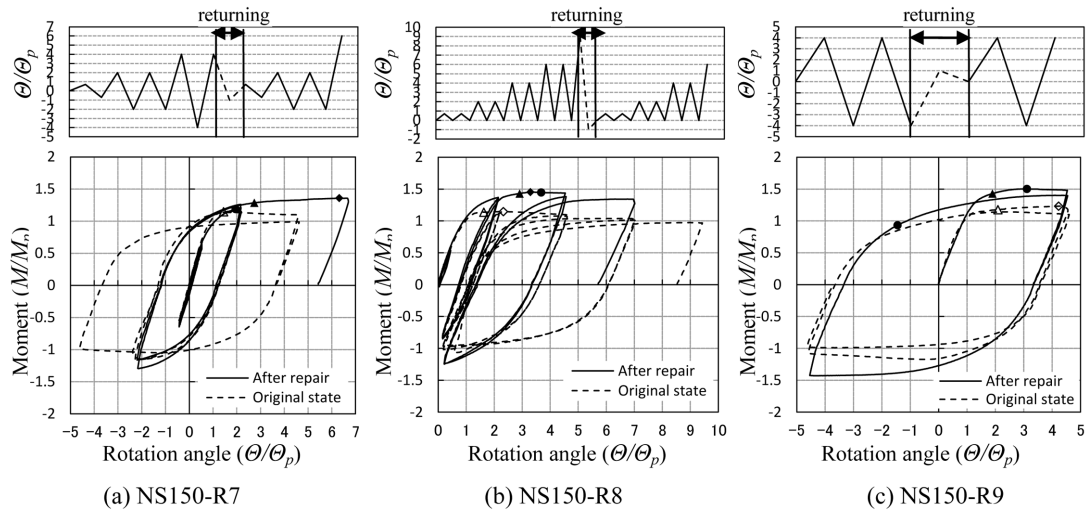

Figure 8. Comparison of normalized $M-\theta$ curve of Cyclic loading of the specimens series 2.

Figure 9. Comparison of normalized $M-\theta$ curve of Cyclic loading of the specimens series 3.

Table 3. Test results

Specimens	First loading			Second loading		
	M_m / M_p	η_m	Failure mode	M_m / M_p	η_m	Failure mode
S110-RM	1.30	3.87		1.57	3.56	Lo.B*
S110-R1	1.26	3.76		1.52	3.50	Crack
S110-R2	1.27	8.07	Lo.B	1.68	11.1	Lo.B
S110-R3	1.23	11.5		1.46	1.42	Crack
S150-RM	1.10	1.40		1.40	2.97	Lo.B
S150-R4	1.12	2.44		1.33	2.71	Crack
S150-R5	1.11	2.00	Lo.B	1.21	2.65	Crack
S150-R6	1.10	1.14		1.30	1.55	Crack
NS150-RM	1.18	2.40		1.40	4.51	Lo.B
NS150-R7	1.16	6.39		1.36	16.5	Crack
NS150-R8	1.15	3.09	Lo.B	1.45	4.24	Lo.B
NS150-R9	1.23	4.07		1.50	2.75	Lo.B

Note: *Lo.B means Local Buckling

strength. Eventually, the load decreased as a crack occurred at the lower area of the cover plate, and this initial crack grew into a major crack in the ultimate state. In the test of specimen S150-RM after repair, it followed the same damaged process as S110-RM, until the load reached maximum strength. After the maximum load, although crack had formed at the lower edge of the welded part between the flange and cover plate, deformation proceeded due to local buckling, and the load decreased gradually.

3.3.2. Cyclic loading

From the results of Figs. 7-9 and Table 3, it is confirmed that the maximum strength is improved by the effect of repair. The strength and ductility before and after repair are compared in Table 4. The energy absorption capacity is assumed to be the energy at the time of maximum strength. From the results of Table 4, it is observed that the increment ratio of maximum strength is over 1.0 times. The increment ratio of the energy absorption capacity generally increases, with some exceptions such as S110-R3 and NS150-R9.

In the case of specimen S110-R3, a welding defect was found at the crack in part to be repaired. Because of this defect, a crack occurred again at the repaired part in the first loop. In the case of the specimen NS150-R9 before repair, the deformation at the flange by the local buckling was unusual, as both sides of the flange near the web deformed towards the inside. Because of this deformation, the ductility capacity until the load reached the maximum strength was larger than that of the other specimens.

4. Analytical Study and Observations

4.1. Analytical model of repaired steel member

Fig. 10 shows photographs of the deformation at the ultimate state of the test specimens. As shown in Fig. 10(a), the area that underwent local buckling before repair has now rotated. As shown in Fig. 10(b), both the area covered

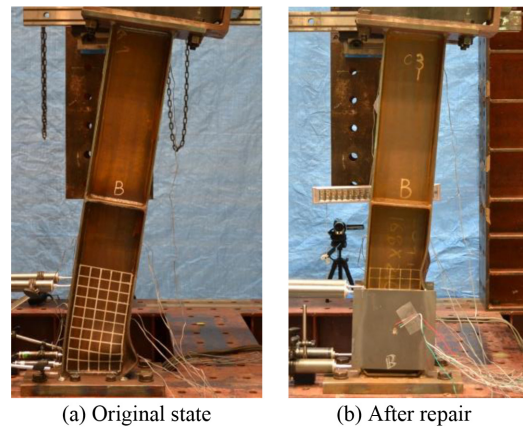


Figure 10. Ultimate state of test specimen.

red by the plate and the upper area of the cover plate have rotated. Fig. 11 illustrates the analytical model of a steel member before and after repair. This analytical model consists of a plastic hinge and a rotational spring, where δ_{hinge} is the displacement of the top of the specimen caused by the rotation of the plastic hinge, and δ_{spring} is the displacement of the top of the specimen caused by the rotation of the rotational spring. In this study, it is defined that both the rotational spring and the plastic hinge have an inelastic restoring force characteristic.

4.2. Restoring force characteristic model

The analytical simulation is conducted using the proposed model of a repaired steel member. The ‘‘Skeleton shift model’’ has been proposed to express the strain hardening or stress degrading phenomena of steel members under cyclic loading (Meng et al., 1992). In this proposed model, an original form of the skeleton curve, composed of a tri-linear curve and hysteresis loops, is expressed by the Ramberg-Osgood function (Ramberg and Osgood, 1943). A special feature of the skeleton shift model is that the skeleton curve may move, depending on the experienced

Table 4. Comparison of strength and ductility before and after repair

Specimens	Maximum strength	Energy absorption capacity
S110-RM	1.21	0.92
S110-R1	1.21	0.93
S110-R2	1.32	1.38
S110-R3	1.19	0.12
S150-RM	1.27	2.12
S150-R4	1.19	1.11
S150-R5	1.09	1.33
S150-R6	1.18	1.36
NS150-RM	1.19	1.88
NS150-R7	1.17	2.58
NS150-R8	1.26	1.37
NS150-R9	1.22	0.68

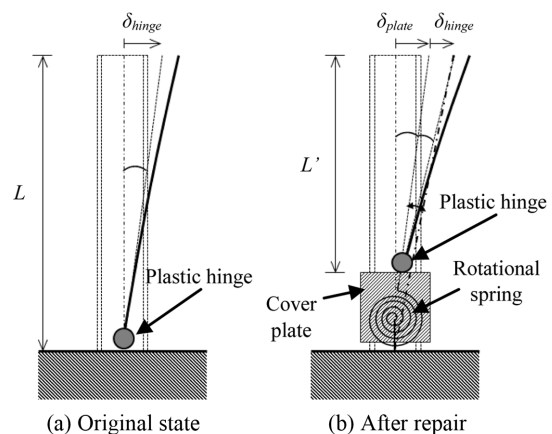


Figure 11. Analytical model before and after repair.

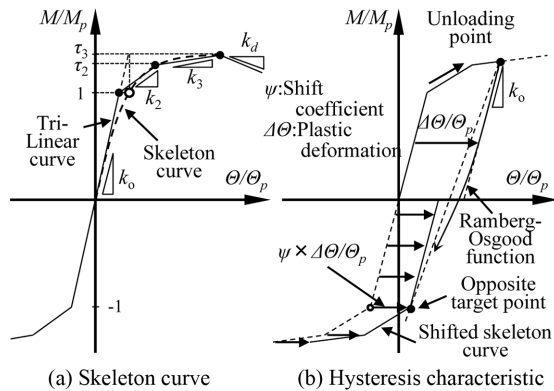

Figure 12. Detail of Skeleton Shift Model.

Table 5. Restoring force and hysteresis characteristics of plastic hinges

Specimens	τ_2	τ_3	k_2	k_3	k_d	ψ	r
Series 1	1.20	1.27	0.13	0.04	-0.03	0.7	8
Series 2	1.04	1.08	0.35	0.06	-0.02	0.7	8
Series 3	1.10	1.14	0.39	0.10	-0.01	0.7	8

Table 6. Restoring force and hysteresis characteristics of rotational springs

Specimens	τ_r	γ	k_r
Series 1	1.2	0.03	
Series 2	1.2	0.03	1, 3, 5, 10
Series 3	1.2	0.03	

plastic strains. A previous study showed that the ultimate behavior of H-shaped steel beams that are subjected to inelastic cyclic loadings can be simulated by applying the restoring force and hysteresis rule of the skeleton shift model to the restoring force characteristic of the beam (Mori and Ito, 2012).

Fig. 12 shows the detail of skeleton shift model. In this study, this model is applied to the plastic hinge. For the rotational spring after repair, bi-linear functions are used as the restoring force characteristics, and the kinematic hardening rule as the hysteresis rule.

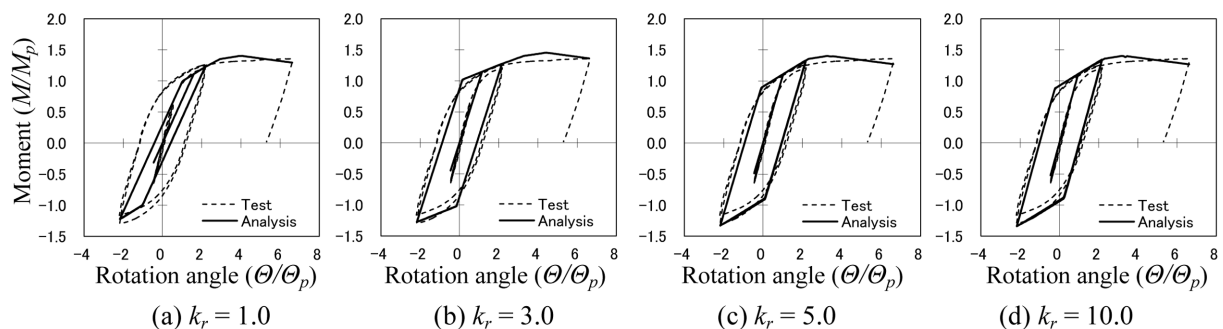
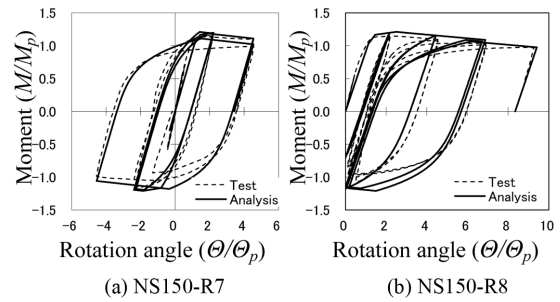

Figure 14. Comparison of normalized $M-\Theta$ curves of test and analytical result of NS150-R7 after repair.

Figure 13. Comparison of normalized $M-\Theta$ curves of test and analytical result before repair.

Table 5 shows the restoring force and hysteresis characteristic of the plastic hinge, fit to the normalized monotonic curve of the test results and the previous study, where r is the coefficient of Ramberg-Osgood function.

Table 6 shows the restoring force and hysteresis of the rotational spring. The rotational spring is simulated with various parameters to study the change in performance (e.g., initial stiffness) of the area covered by the plate. τ_r is the ratio of the yield strength of the plastic hinge to that of the rotational spring, γ is the ratio of second stiffness to initial stiffness of the bi-linear curve, and the analysis parameter k_r is the ratio of the initial stiffness of the rotational spring to that of the plastic hinge.

Fig. 13 compares the normalized $M-\Theta$ curves of specimens NS150-R7 and NS150-R8, obtained from the test and analytical results. Although there are small errors after the loads reach maximum strength, the analytical model can simulate the hysteresis curve of the test results.

Figs. 14 and 15 compare the normalized $M-\Theta$ curves of specimens NS150-R7 and NS150-R8. The analytical results for specimen NS150-R7 shows good agreement with the test results in the range from $k_r=3$ to $k_r=10$. A large rigid rotation of the cover plate was observed, because the ultimate state of specimen NS150-R7 was influenced by cracks that occurred at the flange edge of the lower area of cover plate. For this reason, it is estimated that the rotational spring did not provide a very large rotational stiffness.

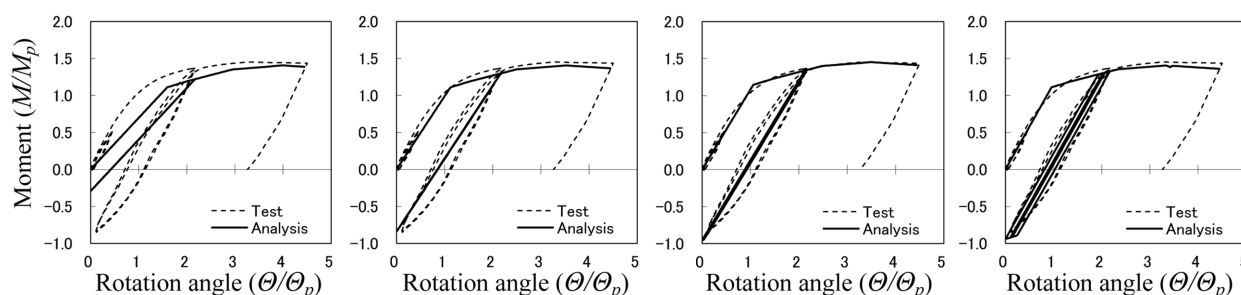


Figure 15. Comparison of normalized $M-\theta$ curves of test and analytical result of NS150-R8 after repair.

Conversely, the analytical results of specimen NS150-R8 show good agreement with the test results at larger values of k_r . In the case of specimen NS150-R8, local buckling that occurred at the upper area of the cover plate caused most of the plastic deformation. Thus, the rotational spring had a large stiffness.

In conclusion, the proposed analytical model can accurately simulate the behavior of repaired members, although consideration of the failure mode is required.

5. Conclusions

This paper focused on repair methods for damaged steel members, and the recoverability of the structural performance of repaired steel structure. In this study, experimental tests were conducted on H-shaped steel members to verify the effects of the repair method, and a simple analytical model for repaired members was presented. To investigate the applicability of the proposed analytical model, an analytical study was conducted.

In the first loading tests, local buckling was observed in all specimens when the load increased, and cracks were observed around scallops after the load reached maximum strength. The second loading tests were conducted after the damage to the test specimens had been repaired. In the second loading tests, it was verified that the maximum strength had increased from the first loading tests. The energy absorption capacity had usually recovered, except in the case of a few specimens.

Furthermore, an analytical model was constructed based on the deformation conditions that were observed during the experimental tests. This model consisted of a plastic hinge and a rotational spring. Static cyclic loading analysis

using this model can accurately simulate the behavior of a repaired test specimen, by applying the appropriate restoring force and hysteresis characteristics. In the case where the ultimate behavior was influenced by local buckling, it was appropriate that a higher stiffness of the rotational spring was established. In the other case, where the ultimate behavior was influenced by cracks that occur at the lower part of the cover plate, it was appropriate that a lower stiffness of the rotational spring was established, because rigid rotation of the cover plate could be distinguished in the experimental test.

References

- The Japan Building Disaster Prevention Association. (2001). *Guideline for Post-Earthquake Damage Evaluation and Rehabilitation Technique* (in Japanese)
- Tanaka, A., Izumi, M., and Narihara, H. (1990). "Experimental Study on the Static Characteristics of Repaired or Reinforced Steel Structures," *Journal of Structural Engineering*, Japan, March, No. 36B, pp. 377~384. (in Japanese).
- Meng, L., Ohi, K., and Takanashi, K. (1992). "A simplified model of steel structural members with strength deterioration used for earthquake response analysis," *Journal of Structural and Construction Engineering*, 437, pp. 115~124.
- Ramberg, W. and Osgood, W. R. (1943). "Description of stress-strain curves by three parameters," National Advisory Committee on Aeronautics. Technical note: 902.
- Mori, K. and Ito, T. (2012). Proposal of hysteresis model and damage evaluation method of steel beams subjected to in elastic cyclic loading, *Proceedings of World Conference on Earthquake Engineering*, Portugal, September.